UV-A Activation of Peroxymonosulfate for the Removal of Micropollutants from Secondary Treated Wastewater

Sonia Guerra-Rodríguez[1], Ana Rita Lado Ribeiro[2,*], Rui S. Ribeiro[2], Encarnación Rodríguez[1], Adrián M.T. Silva[2], Jorge Rodríguez-Chueca[1,*]

(1) Department of Industrial Chemical & Environmental Engineering, Escuela Técnica Superior de Ingenieros Industriales, Universidad Politécnica de Madrid, Madrid, Spain.

(2) Laboratory of Separation and Reaction Engineering – Laboratory of Catalysis and Materials (LSRE-LCM), Faculdade de Engenharia, Universidade do Porto, Rua Dr. Roberto Frias s/n, 4200-465 Porto, Portugal.

*Corresponding authors: jorge.rodriguez.chueca@upm.es (Jorge Rodríguez-Chueca); ritalado@fe.up.pt (Ana Rita Lado Ribeiro).

Abstract

The occurrence of micropollutants (MPs) in the aquatic environment poses a threat for the environment and the human health. The application of advanced oxidation processes based in sulphate radicals (SR-AOPs) to eliminate these contaminants has attracted attention in recent years. In this work, the simultaneous degradation of 20 multi-class MPs (classified into 5 main categories, namely antibiotics, beta-blockers, other pharmaceuticals, pesticides, and herbicides) was evaluated for the first time in secondary treated wastewater, by activating peroxymonosulfate (PMS) by UV-A radiation, without any pH adjustment or iron addition. The optimal PMS concentration to remove the spiked target MPs (100 µg L^{-1}) from wastewater was 0.1 mM, leading to an average degradation of 80% after 60 min, with most of the elimination occurring during the first 5 min. Synergies between radiation and the oxidant were demonstrated and quantified, with an average extent of synergy of 69.1%. The optimized treatment was then tested using non-spiked wastewater, in which 12 out of the 20 target contaminants were detected. Among these, 7 were degraded at some extent, varying from 10.7% (acetamiprid) to 94.4% (ofloxacin), the lower removals being attributed to the quite inferior ratio of MPs to natural organic matter. Phytotoxicity tests carried out with the wastewater before and after photo-activated PMS oxidation revealed a decrease in the toxicity and that the plants were able to grow in the presence of the treated water. Therefore, despite the low degradation rates obtained for some MPs, the treatment effectively reduces the toxicity of the matrix, making the water safer for reuse.

Keywords: UV-A LED radiation; peroxymonosulfate; advanced oxidation process; micropollutants; phytotoxicity.

1. Introduction

The presence of micropollutants (MPs) in the environment is an issue of increasing concern. MPs can be found in aqueous media at concentrations ranging from a few ng L^{-1} to several µg L^{-1} (Luo et al., 2014), most of them being originated in agricultural, domestic, hospital and industrial activities (Sousa et al., 2019). Conventional urban wastewater treatment plants (WWTPs) are not specifically designed to remove this type of organic MPs at trace levels. Thus, the discharge or the reuse of conventionally treated wastewater (still containing MPs) for crop irrigation might pose a risk to the environment and to the human health. In the case of reclaimed water reuse, the remaining chemicals can be uptaken by plants and eventually ingested during food consumption (Delli Compagni et al., 2020). In addition, leaching phenomena can lead to the transfer of contaminants from the soil to groundwater (Valentín et al., 2013).

The proliferation of MPs throughout the environment is particularly worrisome when considering antibiotics. In the last years, increased concerns have been raised on the presence of small amounts of antibiotics, which when sustained over time, promote the development of antibiotic-resistant bacteria and/or resistance genes (ARB&ARGs), thus posing a clear threat to human health (Davies and Davies, 2010). Although the increased awareness towards these issues, there are still very few regulations addressing the presence of MPs in aquatic compartments. The European Union (EU) launched the Water Framework Directive (WFD) (Directive 2000/60/EC, 2000), which sets environmental quality standard (EQS) for 45 priority substances/groups of substances (41 organic compounds and 4 metals). In addition, EU Decision 2015/495 established a watch list of contaminants of emerging concern (CECs) that should be monitored in surface water, although in this case, nor EQS, nor specific regulations were set (Decision 2015/495, 2015). This list has been regularly updated, namely through EU Decisions 2018/840 (Decision 2018/840, 2018) and 2020/1161 (Decision 2020/1161, 2020), the last version including ca. 20 CECs. This watch list has served as reference for various monitoring studies in surface waters (Barbosa et al., 2018; Barreca et al., 2019; Rubirola et al., 2017; Sousa et al., 2018).

Considering that MPs can easily reach the environment through the discharge of inadequately treated wastewater, it is necessary to find alternative treatments able to cope with the removal of MPs. A great variety of different type of treatments has been studied for that purpose, including chemical (Gaya and Abdullah, 2008; Peleyeju and Arotiba, 2018), physical (Kim et al., 2018) and biological (Besha et al., 2017; Grandclément et al., 2017). In this context, the application of advanced oxidation processes (AOPs), based on the generation of highly reactive free radicals, has emerged in the last decades as a great option for the removal of organic contaminants (Gogate and Pandit, 2004; Pera-Titus et al., 2004). The fast reaction rate and strong oxidation capability of these radicals renders them effective for the degradation of several organic MPs in aquatic media (Wang and Zhuan, 2020). Moreover, most AOPs are also effective for the simultaneous inactivation of microorganisms (Rizzo et al., 2019). AOPs are conceptually based on the generation of the hydroxyl radical (HO$^\bullet$), a non-selective and strong oxidant species with a redox potential of +2.8 V, which can destroy the structure of the organic compounds (Mecha et al., 2016). Recently, sulphate radicals (SO$_4^{\bullet-}$) based AOPs have received increasing attention (Liu et al., 2017; Xia et al., 2017; Xie et al., 2019). In comparison to hydroxyl radicals, sulphate radicals possess equal or even higher redox potential (+2.5 to +3.1 V, depending on the activation method), higher selectivity and, in certain cases, longer half-life (Neta et al., 1982). Therefore, sulphate radicals may demonstrate similar or even higher capacity than hydroxyl radicals for the degradation of CECs (Rodríguez-Chueca et al., 2019). They are typically generated from persulfate or peroxymonosulfate (PMS), using different activation methods such as heat (Zrinyi and Pham, 2017), ultraviolet radiation (UV) (Rodríguez-Chueca et al., 2018), ultrasounds (Monteagudo et al., 2018) and/or employing catalysts (Jorge Rodríguez-Chueca et al., 2019; Wei et al., 2016).

UV activation is considered as an environmental friendly and efficient way to activate PMS (Q. Wang et al., 2020), as radicals are generated through two different mechanisms. One possible mechanism is the break of the O-O bond, giving rise to a sulphate radical and a hydroxyl radical (Equation 1). Another mechanism takes place when the radiation excites a water molecule to

98 produce an electron, which activates the PMS by electron conduction (Equations 2-3) (Wang and

99 Wang, 2018).

100 $$HSO_5^- \rightarrow SO_4^{\bullet-} + HO^\bullet \qquad \text{(Equation 1)}$$

101 $$H_2O \rightarrow H^\bullet + HO^\bullet \qquad \text{(Equation 2)}$$

102 $$HSO_5^- + H^\bullet \rightarrow SO_4^{\bullet-} + H_2O \qquad \text{(Equation 3)}$$
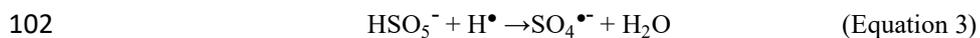
103 The combination of UV-C radiation and PMS has proven to be efficient in the degradation of a

104 large number of pollutants, such as ciprofloxacin (Mahdi-Ahmed and Chiron, 2014),

105 sulphonamides (Cui et al., 2016), imidacloprid (Q. Wang et al., 2020) and di-(2-ethylhexyl)

106 phthalate (Huang et al., 2017). However, the combination of persulfate with UV-A radiation only

107 is less common, an iron-based catalyst being usually added to the treatment. Studies using

108 persulfate/UV-A in wastewater treatment have been focused on the inactivation of

109 microorganisms (Qi et al., 2020; Venieri et al., 2020), or the removal of a single micropollutant,

110 and persulfate (PS) is generally used instead of PMS (Table 1). Therefore, most studies typically

111 deal with the degradation of individual compounds rather than mixtures and/or using ultrapure

112 water as matrix, which is a scenario quite different from that observed in real wastewaters, with

113 complex composition that usually is not taken into account.

114 Bearing this in mind, the main objective of this work is to study, for the first time, the effectiveness

115 of the combination of PMS and UV-A light emitting diodes (LEDs) for the degradation of a wide

116 range of MPs, with diverse chemical nature (Table S1), in a secondary effluent of an urban

117 wastewater treatment plant (WWTP). Accordingly, the performance of the treatment process was

118 first optimized for the simultaneous degradation of 20 multi-class MPs (antibiotics, beta-blockers,

119 other pharmaceuticals, pesticides, and herbicides) spiked in this wastewater, followed by non-

120 spiked experiments with the same water matrix. The MPs under study were selected among those

121 frequently found in wastewater effluents; some of them being included as priority substances in

122 EU Directive 2013/39 and as CECs in EU Decisions 840/2018 and 2020/1161. Phytotoxicity tests

123 were also performed to determine the feasibility and potential of reusing the treated wastewater

124 in crop irrigation.

2. Materials and methods

2.1. Chemicals and materials

The following reference standards (>98 wt.% purity) were acquired from Sigma-Aldrich (Steinhein, Germany): acetamiprid, alachlor, atenolol, atrazine, carbamazepine, ciprofloxacin hydrochloride, enrofloxacin, erythromycin, isoproturon, methiocarb, metoprolol tartrate, ofloxacin, propranolol, simazine, tetracycline hydrochloride, thiacloprid, thiamethoxam, tramadol hydrochloride, trimethoprim, and warfarin. The isotopically labelled internal standards (i.e., acetamiprid-d3, azithromycin-d5, atrazine–d5, diclofenac-d4, ketoprofen–d3, methiocarb-d3, propranolol-d7, and ofloxacin-d3) were supplied by Sigma-Aldrich (Steinheim, Germany). Acetonitrile (MS grade) and ethanol (EtOH; HPLC grade) were purchased to VWR International (Fontenay-sous-Bois, France). Peroxymonosulfate (PMS; $2 \cdot KHSO_5 \cdot KHSO_4 \cdot K_2SO_4$), formic and sulphuric acid (H_2SO_4) were obtained from Merck (Darmstadt, Germany). Disodium hydrogen phosphate (Na_2HPO_4; 99 wt.%), monosodium phosphate (NaH_2PO_4; 99 wt.%), and N, N-Dietyl-p-phenylenediamine sulphate (DPD; 99 wt.%) were obtained from Fluka (Seelze, Germany). Ultrapure water was supplied by a Milli-Q water system. A stock solution containing the 20 organic MPs (100 mg L^{-1} each) was prepared by dissolution of the reference standards in EtOH.

2.2. Secondary treated wastewater

The water matrix used in all the experiments was collected from the secondary effluent of an urban WWTP located in northern Portugal. The treated wastewater (WW) sample, whose properties are summarized in Table 2, was divided into aliquots and filtered through 1.2 μm glass-fibre filters (47 mm GF/C, Whatman™, Maidstone, United Kingdom) under vacuum to remove suspended solids. The aliquots were stored in the freezer to preserve its properties until usage. The content of trace elements in the WW sample was also analysed (Table S2).

2.3. Experimental set-up

149   All the experiments (spiked and non-spiked) were performed with secondary treated wastewater,

150   without pH adjustment (natural pH), in a 1 L cylindrical glass reactor under magnetic stirring, to

151   ensure the homogeneity of the solution. Four LEDs emitting in the UV-A region were used (λ_{max}

152   = 385 nm) for the activation of PMS. Each LED was equipped with an electric fan to avoid

153   overheating and placed at the same distance of the reactor in 4 walls of a metallic cubic support,

154   the schematic representation of the experimental set-up being shown elsewhere (Biancullo et al.,

155   2019). The PMS dosage (0.05, 0.1 or 0.5 mM) was initially optimized. In these experiments, 1

156   mL of stock solution was added into the reactor to reach a concentration of 100 µg L^{-1} of each

157   MP, the ethanol being evaporated with a nitrogen stream until dryness. The evaporation of ethanol

158   aimed to avoid its scavenging effect on sulphate and/or hydroxyl radicals. After drying, 1 L of

159   wastewater was added to the reactor, which was left for 2 min in an ultrasonic bath to enable the

160   solubilisation of the MPs in the wastewater. Each experiment started after 5 min of stirring under

161   dark conditions, upon collection of the first sample. Once the first sample was collected, a known

162   amount of PMS was added to the solution and the LEDs were turned on ($t_0 = 0$). A volume of 400

163   µL was sampled at 0, 5, 10, 20, 30 and 60 min, and refrigerated until analysis.

164   Non-spiked experiments were also performed, using a PMS dosage of 0.1 mM. In this case, solid-

165   phase extraction (SPE) was performed, as described in Section 2.4.1, to concentrate the samples

166   prior to analysis.

167   *2.4. Analytical methods*

168   *2.4.1. Solid-phase extraction*

169   Each sample collected in the non-spiked experiments (100 mL) was acidified (pH = 2) with H_2SO_4

170   and spiked with 50 µL of the stock solution of internal standards. According to the SPE procedure

171   described by Ribeiro et al. (2015), OASIS® HLB cartridges (150 mg, 6 mL) were conditioned

172   sequentially with 4 mL of EtOH and 4 mL of acidified ultrapure water (pH = 3) at a flow rate of

173   1 mL min^{-1}. Then, the cartridges were loaded with each sample at a constant flow rate of

174   10mLmin^{-1}. After washing with 4 mL of a 5% ethanolic solution in ultrapure water, the cartridges

175 were dried under vacuum for 30 min. The elution was performed with 4 mL EtOH at 1mL min^{-1}

176 to extract the target analytes. The extracts were evaporated to dryness in a Centrivap

177 Concentrator® device (LABCONCO® Corporation, Kansas City, MO, USA), and the residues

178 were dissolved in 250 μL of EtOH and filtered through 0.22 μm polytetrafluoroethylene (PTFE)

179 syringe filters (Membrane Solutions, Texas, USA) prior to the chromatographic analysis

180 described in Section 2.4.2. A pH meter pHenomenal® pH 1100L (VWR, Germany) was used for

181 pH adjustments.

182 *2.4.2. Liquid Chromatography-tandem Mass Spectrometry*

183 The concentration of each analyte was analysed in triplicate using an ultra-high performance

184 liquid chromatography with tandem mass spectrometry (UHPLC-MS/MS) Shimadzu Corporation

185 apparatus (Japan) consisting of a UHPLC equipment (Nexera) coupled to a triple quadrupole mass

186 spectrometer (Ultra Fast Mass Spectrometry series LCMS-8040), with an ESI source operating

187 in both positive and negative ionisation modes. A Kinetex™ 1.7 μm XB-C18 100 Å column (100

188 × 2.1 mm i.d.) (Phenomenex, Inc., California, USA) was used, with a mobile phase consisting of

189 an aqueous solution of formic acid (0.1%) and acetonitrile, under gradient mode, with the

190 temperature of the column oven set to 35 °C. The volume of injection was 10 μL and the

191 autosampler temperature was kept at 4 °C. The quantification of the target compounds was

192 performed by selected reaction monitoring (SRM), using the most abundant fragment ion as

193 quantifier and the second most abundant for confirmation of the identity. The optimized

194 parameters, capillary voltage, drying gas and nebulizing gas flows, desolvation and source

195 temperatures were respectively: 4.5 kV, 15 dm^3 min^{-1}, 3.0 dm^3 min^{-1}, 400 °C and 250 °C. The

196 collision induced dissociation gas (CID) was argon at 230 kPa.

197 *2.4.3. Dissolved organic carbon determination*

198 Dissolved organic carbon (DOC) was determined following the standard procedure 5310 B of the

199 Standard Methods for Examination of Water and Wastewater (APHA et al., 1988), and using a

200 Shimadzu TOC-L apparatus.

2.4.4. PMS monitoring

A colorimetric method with N,N-diethyl-p-phenylenediamine (DPD) was used to monitor the consumption of PMS (Vieira et al., 2020). Briefly, a phosphate buffer (pH 7) composed of Na_2HPO_4 and NaH_2PO_4 in ultrapure water (H_2O_{UP}), and a DPD solution (25 mM) in H_2SO_4 (0.05M) were prepared. Once the phosphate buffer and the DPD solution were added to the sample, the colour was allowed to develop during 10 min at room temperature and the absorbance was measured at 551 nm against a blank prepared with ultrapure water.

2.4.5. Phytotoxicity tests

The phytotoxicity of the wastewater was assessed prior and after photo-activated PMS oxidation performed under optimized conditions. For that purpose, phytotoxicity tests (Phytotestkit microbiotest; MicroBioTests Inc.) were performed in triplicate. These tests comply with ISO Standard 18763 and allow evaluating the germination and growth of three different plants (*Sorghum saccharatum*, *Lepidium sativum*, and *Sinapis alba*). The number of germinated seeds was determined, and the roots and stems were measured after 3 days of incubation at 25 ºC. ImageJ software was used for image processing.

Growth increase (%) was calculated for stems and roots of each species. This parameter was obtained following Equation 4, where L_T and L_{NT} represents the average length of roots/stems of plants germinated in treated and non-treated wastewater, respectively.

$$\text{Growth (\%)} = \frac{L_T - L_{NT}}{L_T} \times 100 \qquad \text{(Equation 4)}$$

2.5. Extent of synergy

In order to quantify the possible synergistic effect taking place in the treatments, the extent of synergy (S) was calculated for each MP. For that, all the pseudo–first order kinetic constants (k) were previously determined. Once calculated, S was obtained from Equation 5 (Zanias et al., 2020).

$$S\ (\%) = \frac{k_{PMS+UV-A} - k_{PMS} - k_{UV-A}}{k_{PMS+UV-A}} \times 100 \qquad \text{(Equation 5)}$$

3. Results

3.1. Experiments with spiked MPs

Experiments were first performed with secondary treated wastewater spiked with the 20 organic MPs under study at a concentration of 100 µg L^{-1} each. The main goal was to optimize the PMS dosage employed in the photo-activated oxidation process. For that purpose, photo-activation of PMS was carried out with three different dosages of the oxidant source, namely 0.05, 0.1 and 0.5 mM. A remarkable increase in MPs removals was achieved when the PMS dosage increased from 0.05 to 0.1 mM (**Figure 1**). Specifically, the average removal of the selected MPs increases from 31.8% when using 0.05 mM of PMS, to 87.4% when employing 0.1 mM of PMS. Although increasing the PMS concentration further (to 0.5 mM) led to a more pronounced degradation of some pollutants (e.g., trimethoprim, the 3 beta-blockers, tramadol, warfarin, and thiacloprid), the average MPs removal was slightly lower (82%) than that obtained with 0.1 mM of PMS. This effect may be due to the fact that excess PMS can scavenge the generated hydroxyl and sulphate radicals (Equations 6-7), which originate less reactive species as well as their recombination (Equations 8-10) (Khan et al., 2017). These phenomena have been reported on several occasions when combining PMS with UV radiation. For example, concentrations of PMS above 0.66 mM were reported to decrease the treatment performance for the elimination of Bisphenol A (Sharma et al., 2015). The same effect was observed by Jiang et al. (2018) for the removal of refractory pollutants in incineration leachate. Therefore, 0.1 mM was selected as the optimum PMS dosage, and employed in subsequent experiments.

$SO_4^{\bullet-} + HSO_5^- \rightarrow SO_5^{\bullet-} + SO_4^{2-} + H^+$ ($k < 1.0 \times 10^5$ M^{-1}s^{-1}) (Brandt and Eldik, 1995) (Equation 6)

$OH^{\bullet} + HSO_5^- \rightarrow SO_5^{\bullet-} + H_2O$ (Neta et al., 1988)   (Equation 7)

$SO_4^{\bullet-} + SO_4^{\bullet-} \rightarrow S_2O_8^{2-}$ ($k = 4.0 \times 10^8$ M^{-1}s^{-1})   (Huie and Clifton, 1993) (Equation 8)

$OH^{\bullet} + SO_4^{\bullet-} \rightarrow HSO_5^-$ ($k = (0.95 \pm 0.08) \times 10^{10}$ M^{-1}s^{-1})   (Khan et al., 2017)   (Equation 9)

$OH^{\bullet} + OH^{\bullet} \rightarrow H_2O_2$ ($k = 5.3 \times 10^9$ M^{-1}s^{-1})   (Khan et al., 2017)   (Equation 10)
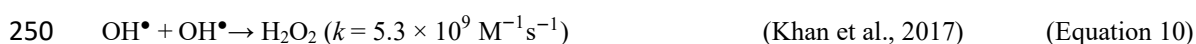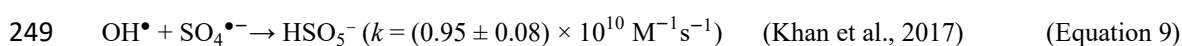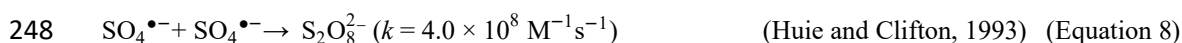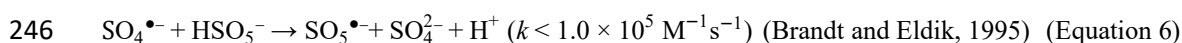
Complementary experiments were performed to discriminate the different contributions for the degradation of each MP by photo-activated PMS oxidation, namely photolysis and PMS

oxidation. Both processes may be taking place during treatment and their effects may be additive or synergistic, the latter being the desirable scenario. The degradation of the target MPs promoted by photolysis (i.e., by UV-A radiation only) was first evaluated. In this work the treatments were tested with real wastewater so both direct and indirect photolysis are expected to take place [43, 44]. Apart from direct degradation of the MPs due to the electronic excitation of the molecules, compounds dissolved in the matrix may contribute to the degradation since reactive oxygen species can be originated by the irradiation of photosensitizers dissolved in the water matrix (Lado Ribeiro et al., 2019). However, dissolved organic matter is also responsible for irradiation absorption, diminishing the degradation by direct radiation. As observed, the effect of UV-A radiation on the degradation of most of the target MPs is negligible (**Figure 2a**). Indeed, after 60min of reaction, most of the contaminants were removed by less than 15% with UV-A, except tetracycline, propranolol, atrazine, thiacloprid, and methiocarb, for which removals of 97%, 26%, 35%, 24%, and 52% were respectively obtained. The contribution of PMS oxidation for the degradation of each MP was also studied. For 11 out of the 20 target MPs, a degradation lower than 35% was verified after 60 min of reaction under dark. However, 6 out of the 20 target pollutants (all the antibiotics and methiocarb) were completely degraded. This fact suggests that PMS oxidation plays a remarkable role in the degradation of these 6 MPs in the real matrix studied.

When comparing the results obtained for the treatments involving only PMS or UV-A radiation with those observed after treatment by PMS/UV-A, a noteworthy improvement in the removal of most compounds was observed by photo-activation of PMS. This effect is especially remarkable in the case of the most recalcitrant compounds when using PMS or UV-A radiation alone, i.e. atenolol, alachlor, acetamiprid, isoproturon, simazine, carbamazepine, and thiamethoxam. For the last 4 compounds cited, a negligible degradation was observed by adding PMS in the dark and during photolysis, but around 80% of elimination was achieved with the combined treatment. In order to quantify the possible synergistic effect taking place, the extent of synergy (S) was calculated and plotted for each MP (**Figure 2b)**. This analysis was not performed for

ciprofloxacin, erythromycin, enrofloxacin, ofloxacin, methiocarb, and tetracycline, due to the lack of data. In fact, these compounds were removed in less than 5 min in the experiments carried out with PMS/UV-A, thus precluding the determination of their pseudo-first order kinetic constants. Furthermore, these MPs were those fully degraded with PMS (dark). The S values obtained for the studied MPs are consistent with the results given in Figure 2a. As expected, no synergies were found between the oxidant and UV-A radiation for the degradation of thiacloprid and warfarin, since in these cases, the sum of the single effect of UV-A and PMS was equal to that obtained from their combined use. Moreover, only 3% of synergy extent was estimated for tramadol, which was not degraded by single UV-A. A completely different situation was observed for the other MPs, for which an average S of 87.6% was obtained. The value of S drops to 69.1% when considering all the 20 MPs under study. These results confirm the existence of synergies between PMS and the applied UV-A radiation, possibly due to the enhanced formation of radicals. This phenomenon has been previously reported for the degradation of other pollutants under UV-C irradiation. Zhang et al., (2019) showed that the degradation of haloacetonitriles was practically non-existent when using UV-C or PMS (individually) in deionized water. However, when UV-C was combined with PMS, the degradation increased to 80% in just 30 min. The same has been observed when using this treatment in the degradation of tris(2-chloroethyl) phosphate (TCEP) in ultrapure water. In another study (Xu et al., 2017), it was determined that the elimination of this compound was 94.6% after 30 min of treatment with a [PMS]:[TCEP] ratio of 20:1 under UV-C radiation, while negligible degradation was obtained by PMS oxidation, and only 4.5% was removed by photolysis.

In order to understand if there is any similar trend in the degradation kinetics obtained for each particular class of MPs, the 20 compounds under study were grouped into 5 main categories, namely antibiotics, beta-blockers and other pharmaceuticals (anticoagulant, analgesic and anticonvulsant), herbicides, and insecticides. The degradation kinetics obtained for each class was then analysed (**Figure 3**). As observed, all antibiotics (**Figure 3a)** are degraded within 5 minutes (when the first sample was collected), except for trimethoprim. This suggests that the target

antibiotics are degraded by PMS/UV-A (or even PMS, **Figure 2a**), which may be transformed in

by-products or even mineralized. These results differ from those obtained by other authors for the

degradation of ciprofloxacin (Ao et al., 2018) and tetracycline (Ao et al., 2019) in milli-Q water

under UV-C radiation (pH = 3.7). In those studies, the degradation of the antibiotics was

negligible when using only PMS, being lower when combining PMS and UV-C radiation than in

the present study. However, Ao et al. (2019) reported higher removals of TC in real matrices

collected from different drinking water treatment plants, which was ascribed to other water

constituents in real water matrices, either inorganic or organic that can act as a promoters or

inhibitors of radicals. Some studies suggest that the presence of carbonates, nitrates or chlorides

in the medium can improve the effectiveness of the treatment (Ao et al., 2018), while the presence

of organic matter inhibits the degradation of pollutants (Q. Wang et al., 2020). However, there is

no agreement between the authors, the effects of each of these components being different

depending on the target pollutant and the overall composition of the matrix. Similarly to

antibiotics, all beta-blockers followed similar degradation kinetics **(Figure 3b)**, with a fast

elimination within the first 5 min of reaction, after which a residual removal occurred until 30min

of reaction, when ca. 86% of the compounds was eliminated. For the other three pharmaceuticals

not included in these therapeutic classes **(Figure 3c)**, 83% and 90% of tramadol and warfarin

were degraded after 10 min, respectively. By contrast, 59.5% of carbamazepine was removed in

the same period of time. Compared to pharmaceuticals, herbicides **(Figure 3d)** and insecticides

(Figure 3e) were more recalcitrant, except the insecticide methiocarb that had similar kinetic to

that observed for antibiotics, indicating its complete removal. Once again, the most intense

reduction was observed during the first 5 minutes (48-64%) and the reaction seemed to stop after

30 minutes, with an elimination of 71-82%, the amount of pesticides remaining in the water being

nearly 2-fold greater than that of the beta-blockers.

Interestingly, the decay of PMS is similar to that observed for the target MPs, with 32% of the

PMS being consumed during the first 5 min of reaction, while additional 11% were consumed in

334 30 min (**Figure 4**). At the end of the experiments, 50% of the initial PMS was consumed, from

335 which only 7% was consumed in the second half-hour.

336 In order to evaluate the possible effect of residual EtOH (a well-known scavenger of hydroxyl

337 and sulphate radicals) in the reactor, resulting from residues that could persist in the evaporation

338 step after spiking the stock solution, and to get insights about the possible pathways (radical

339 and/or non-radical), an experiment was performed without EtOH evaporation. **Figure 5** shows a

340 marked reduction in the removal of most of the MPs in the presence of the alcohol, the degradation

341 results being comparable to those obtained with non-activated PMS oxidation. This observation

342 confirms the generation of radicals during PMS photo-activation. More experiments would be

343 necessary to determine which of these two radical species is responsible for the degradation of

344 the pollutants, but this subject falls out of the goal of this study. Nevertheless, our results are in

345 agreement with some reports on the simultaneous occurrence of radical and non-radical

346 degradation pathways in activated PMS oxidation of organic MPs (C. Li et al., 2019; W. Li et al.,

347 2019; Xu et al., 2020).

348

349 ***3.2. Non-spiked experiments***

350 *3.2.1. Degradation results*

351 Once the optimum PMS dosage was determined (**Figure 1**), the effectiveness of the treatment to

352 eliminate the MPs originally present in the wastewater (without spiking) was studied. For this

353 purpose, a wastewater sample previously concentrated using the SPE procedure described in

354 Section 2.4.1, was analysed to find out which of the pollutants targeted in this study can be found

355 in the collected effluent. 12 out of 20 target contaminants were detected in the actual wastewater.

356 Interestingly, these MPs were those most recalcitrant to the proposed treatment (**Figure 2**).

357 A treatment time of 30 min was selected for the experiments in non-spiked wastewater (Table 3),

358 considering the results obtained in the spiked experiments (**Figure 3**), i.e. no remarkable

359 degradation is expected afterwards.

Among the MPs detected, 5 were not degraded (carbamazepine, warfarin, simazine, thiamethoxan, and trimethoprim). The remaining were removed to a greater or lesser extent, varying from 10.7% (acetamiprid) to 94.4% (ofloxacin), the average degradation being 28.9%. This value differs from the results obtained in the spiked experiments, where more than 80% of the pollutants were degraded under the same conditions, suggesting that the removal achieved increases with pollutant concentration in the range considered in this study (up to 100 $\mu g\ L^{-1}$), i.e. a higher removal is achieved when the mass ratio of MPs to natural organic matter is higher. Although this phenomenon cannot be completely understood based on our results, the observations herein reported highlight the importance of carrying out future studies under realistic conditions. Otherwise, misleading conclusions may limit potential improvements of this treatment technology.

At the moment, very few research articles have been published in the application of this treatment to the degradation of such a high number of compounds at the same time. Rodríguez-Chueca et al. (2018) studied the degradation of 25 compounds of different classes in real wastewater, achieving an average removal of 48%, which is higher than that observed in the present study (28.9%). This higher performance can be explained by the use of UV-C radiation in that research, which is a better PMS activator than UV-A here reported. Moreover, the use of a higher concentration of PMS was also described (0.5 mM versus 0.1 mM, in the present study).

3.2.2. Phytotoxicity assessment

Phytotoxicity assays were carried out to assess the possible increase on toxicity after treatment, due to either the formation of toxic by-products resulting from the degradation of the target contaminants or the presence of PMS does. As is shown in **Table 4**, almost all the seeds germinated in both treated and untreated wastewater. However, **Figure 6** shows that in all cases the plants have grown more when fed with treated wastewater (instead of untreated wastewater), the roots and the shoots being 18% and 27% longer on average, respectively. The main difference was observed for *Lepidium sativum*, where the roots and the shoots grew on average 22% and 31% more, respectively.

Phytotoxicity tests are rare when studying this type of treatment and there are many different species that can be used for this purpose. However, some authors have found that treatments based on sulphate radicals can reduce phytotoxicity (Ghanbari et al., 2020; Jaafarzadeh et al., 2017), which is confirmed by the results herein presented. This is an advantage of this treatment over others, which may not reduce toxicity. For instance, with similar phytotoxicity tests, it has been reported that treatments that use ozone to eliminate pollutants tend to increase the toxicity of the water, possibly due to the greater toxicity of the oxidation products generated than that of the original matrix (Iakovides et al., 2019). Our work demonstrated that the proposed treatment does not increase the toxicity of the effluents, it actually reduces the pre-existing levels.

4. Conclusions

A PMS/UV-A treatment was successful applied for the degradation of 20 multi-class MPs spiked in real wastewater. Nearly half of the optimal concentration (0.1 mM) of the oxidant was consumed in the first 30 min of reaction, which was accompanied by the elimination of ca. 80% of the initial concentration of the spiked MPs. In general, the herbicides and pesticides were more recalcitrant to the PMS/UV-A process than pharmaceuticals. The existence of synergies between the oxidant and the UV-A radiation was estimated as 69.1%, which might be related to the formation of additional radicals with PMS/UV-A. The degradation of 12 MPs detected in the collected wastewater varied between 0% and 94.4%, with an average removal (28.9%) considerably lower than that obtained in the spiked experiments. The drop in the efficiency of the treatment showcases the critical importance of conducting future studies under realistic conditions. Moreover, phytotoxicity assays revealed a decrease in the toxicity of the wastewater after treatment. Specifically, the roots and the shoots of the germinated seeds were 18% and 27% longer on average, respectively, when they were fed with treated wastewater instead of fresh wastewater. Therefore, the proposed treatment reduces the pre-existing toxicity, allowing for a

412 safer water reuse. This is an advantage over other treatments that have been shown to generate

413 toxic by-products.

414

429

430 **5. References**

431 Ao, X., Liu, W., Sun, W., Cai, M., Ye, Z., Yang, C., Lu, Z., Li, C., 2018. Medium pressure UV-

432   activated peroxymonosulfate for ciprofloxacin degradation: Kinetics, mechanism, and

433   genotoxicity. Chem. Eng. J. 345, 87–97. https://doi.org/10.1016/j.cej.2018.03.133

434 Ao, X., Sun, W., Li, S., Yang, C., Li, C., Lu, Z., 2019. Degradation of tetracycline by medium

435   pressure UV-activated peroxymonosulfate process: Influencing factors, degradation

436   pathways, and toxicity evaluation. Chem. Eng. J. 1053–1062.

437   https://doi.org/10.1016/j.cej.2018.12.133

438   APHA, AWWA, WEF, 1988. Standard Methods for the Examination of Water and Wastewater.

439   Arslan-Alaton, I., Kolba, O., Olmez-Hanci, T., 2018. Removal of an X-Ray contrast chemical

440   from tertiary treated wastewater: Investigation of persulfate-mediated photochemical

441   treatment systems. Catal. Today 313, 134–141.

442   https://doi.org/10.1016/j.cattod.2017.11.002

443   Barbosa, M.O., Ribeiro, A.R., Ratola, N., Hain, E., Homem, V., Pereira, M.F.R., Blaney, L.,

444   Silva, A.M.T., 2018. Spatial and seasonal occurrence of micropollutants in four

445   Portuguese rivers and a case study for fluorescence excitation-emission matrices. Sci.

446   Total Environ. 644, 1128–1140. https://doi.org/10.1016/j.scitotenv.2018.06.355

447   Barreca, S., Busetto, M., Colzani, L., Clerici, L., Daverio, D., Dellavedova, P., Balzamo, S.,

448   Calabretta, E., Ubaldi, V., 2019. Determination of estrogenic endocrine disruptors in water

449   at sub-ng L −1 levels in compliance with Decision 2015/495/EU using offline-online solid

450   phase extraction concentration coupled with high performance liquid chromatography-

451   tandem mass spectrometry. Microchem. J. 147, 1186–1191.

452   https://doi.org/10.1016/j.microc.2019.04.030

453   Besha, A.T., Gebreyohannes, A.Y., Tufa, R.A., Bekele, D.N., Curcio, E., Giorno, L., 2017.

454   Removal of emerging micropollutants by activated sludge process and membrane

455   bioreactors and the effects of micropollutants on membrane fouling: A review. J. Environ.

456   Chem. Eng. https://doi.org/10.1016/j.jece.2017.04.027

457   Biancullo, F., Moreira, N.F.F., Ribeiro, A.R., Manaia, C.M., Faria, J.L., Nunes, O.C., Castro-

458   Silva, S.M., Silva, A.M.T., 2019. Heterogeneous photocatalysis using UVA-LEDs for the

459   removal of antibiotics and antibiotic resistant bacteria from urban wastewater treatment

460   plant effluents. Chem. Eng. J. 367, 304–313. https://doi.org/10.1016/j.cej.2019.02.012

461   Brandt, C., Eldik, R. Van, 1995. Transition Metal-Catalyzed Oxidation of Sulfur (lV) Oxides .

462   Atmospheric-Relevant Processes and Mechanisms. Chem. Rev. 119–190.

463   Cui, C., Jin, L., jiang, L., Han, Q., Lin, K., Lu, S., Zhang, D., Cao, G., 2016. Removal of trace

464   level amounts of twelve sulfonamides from drinking water by UV-activated

465   peroxymonosulfate. Sci. Total Environ. 572, 244–251.

466   https://doi.org/10.1016/j.scitotenv.2016.07.183

467   Davies, J., Davies, D., 2010. Origins and evolution of antibiotic resistance. Microbiol. Mol.

468   Biol. Rev. 74, 417–433. https://doi.org/10.1128/MMBR.00016-10

469   Decision 2015/495, 2015. Commission Implementing Decision (EU) 2015/495 of 20 March

470   2015 establishing a watch list of substances for Union-wide monitoring in the field of

471   water policy pursuant to Directive 2008/105/EC of the European Parliament and of the

472   Council.

473   Decision 2018/840, 2018. Commision Implementing Decision (EU) 2018/840 of 5 June 2018

474   establishing a watch list of substances for Union-wide monitoring in the field of water

475   policy pursuant to Directive 2008/105/EC of the European Parliament and of the Council

476   and repealing Commi.

477   Decision 2020/1161, 2020. Commission Implementing Decision (EU) 2020/1161 of 4 August

478   2020 establishing a watch list of substances for Union-wide monitoring in the field of

479   water policy pursuant to Directive 2008/105/EC of the European Parliament and of the

480   Council.

481   Delli Compagni, R., Gabrielli, M., Polesel, F., Turolla, A., Trapp, S., Vezzaro, L., Antonelli,

482   M., 2020. Risk assessment of contaminants of emerging concern in the context of

483   wastewater reuse for irrigation: An integrated modelling approach. Chemosphere 242,

484   125185. https://doi.org/10.1016/J.CHEMOSPHERE.2019.125185

485   Directive 2000/60/EC, 2000. Directive 2000/60/EC of the European Parliament and of the

486   Council of 23 October 2000 establishing a framework for Community action in the field of

487   water policy. Off. J. L 327.

488   Gaya, U.I., Abdullah, A.H., 2008. Heterogeneous photocatalytic degradation of organic

489   contaminants over titanium dioxide: A review of fundamentals, progress and problems. J.

490   Photochem. Photobiol. C Photochem. Rev.

491   https://doi.org/10.1016/j.jphotochemrev.2007.12.003

492   Ghanbari, F., Wu, J., Khatebasreh, M., Ding, D., Lin, K.Y.A., 2020. Efficient treatment for

493   landfill leachate through sequential electrocoagulation, electrooxidation and

494   PMS/UV/CuFe2O4 process. Sep. Purif. Technol. 242, 116828.

495   https://doi.org/10.1016/j.seppur.2020.116828

496   Giannakis, S., Gamarra Vives, F.A., Grandjean, D., Magnet, A., De Alencastro, L.F., Pulgarin,

497   C., 2015. Effect of advanced oxidation processes on the micropollutants and the effluent

498   organic matter contained in municipal wastewater previously treated by three different

499   secondary methods. Water Res. 84, 295–306. https://doi.org/10.1016/j.watres.2015.07.030

500   Gogate, P.R., Pandit, A.B., 2004. A review of imperative technologies for wastewater treatment

501   I: Oxidation technologies at ambient conditions. Adv. Environ. Res. 8, 501–551.

502   https://doi.org/10.1016/S1093-0191(03)00032-7

503   Grandclément, C., Seyssiecq, I., Piram, A., Wong-Wah-Chung, P., Vanot, G., Tiliacos, N.,

504   Roche, N., Doumenq, P., 2017. From the conventional biological wastewater treatment to

505   hybrid processes, the evaluation of organic micropollutant removal: A review. Water Res.

506   https://doi.org/10.1016/j.watres.2017.01.005

507   Huang, J., Li, X., Ma, M., Li, D., 2017. Removal of di-(2-ethylhexyl) phthalate from aqueous

508   solution by UV/peroxymonosulfate: Influencing factors and reaction pathways. Chem.

509   Eng. J. 314, 182–191. https://doi.org/10.1016/J.CEJ.2016.12.095

510   Huang, W., Bianco, A., Brigante, M., Mailhot, G., 2018. UVA-UVB activation of hydrogen

511   peroxide and persulfate for advanced oxidation processes: Efficiency, mechanism and

512   effect of various water constituents. J. Hazard. Mater. 347, 279–287.

513   https://doi.org/10.1016/j.jhazmat.2018.01.006

514   Huie, R.E., Clifton, C.L., 1993. Kinetics of the self-reaction of hydroxymethylperoxyl radicals.

515   Chem. Phys. Lett. 205, 163–167. https://doi.org/10.1016/0009-2614(93)89222-4

516   Iakovides, I.C., Michael-Kordatou, I., Moreira, N.F.F., Ribeiro, A.R., Fernandes, T., Pereira,

517   M.F.R., Nunes, O.C., Manaia, C.M., Silva, A.M.T., Fatta-Kassinos, D., 2019. Continuous

518   ozonation of urban wastewater: Removal of antibiotics, antibiotic-resistant Escherichia

519   coli and antibiotic resistance genes and phytotoxicity. Water Res. 159, 333–347.

520   https://doi.org/10.1016/j.watres.2019.05.025

521   Ioannidi, A., Frontistis, Z., Mantzavinos, D., 2018. Destruction of propyl paraben by persulfate

522   activated with UV-A light emitting diodes. J. Environ. Chem. Eng. 6, 2992–2997.

523   https://doi.org/10.1016/j.jece.2018.04.049

524   Jaafarzadeh, N., Ghanbari, F., Ahmadi, M., Omidinasab, M., 2017. Efficient integrated

525   processes for pulp and paper wastewater treatment and phytotoxicity reduction:

526   Permanganate, electro-Fenton and Co3O4/UV/peroxymonosulfate. Chem. Eng. J. 308,

527   142–150. https://doi.org/10.1016/j.cej.2016.09.015

528   Jiang, F., Qiu, B., Sun, D., 2018. Advanced degradation of refractory pollutants in incineration

529   leachate by UV/Peroxymonosulfate. Chem. Eng. J. 349, 338–346.

530   Khan, S., He, X., Khan, J.A., Khan, H.M., Boccelli, D.L., Dionysiou, D.D., 2017. Kinetics and

531   mechanism of sulfate radical- and hydroxyl radical-induced degradation of highly

532   chlorinated pesticide lindane in UV/peroxymonosulfate system. Chem. Eng. J. 318, 135–

533   142. https://doi.org/10.1016/j.cej.2016.05.150

534   Kim, S., Chu, K.H., Al-Hamadani, Y.A.J., Park, C.M., Jang, M., Kim, D.-H., Yu, M., Heo, J.,

535   Yoon, Y., 2018. Removal of contaminants of emerging concern by membranes in water

536   and wastewater: A review. Chem. Eng. J. 335, 896–914.

537   https://doi.org/10.1016/J.CEJ.2017.11.044

538   Lado Ribeiro, A.R., Moreira, N.F.F., Li Puma, G., Silva, A.M.T., 2019. Impact of water matrix

539   on the removal of micropollutants by advanced oxidation technologies. Chem. Eng. J. 363,

540   155–173. https://doi.org/10.1016/j.cej.2019.01.080

541   Legrini, O., Oliveros, E., Braun, A.M., 1993. Photochemical Processes for Water Treatment.

542   Chem. Rev. 93, 671–698. https://doi.org/10.1021/cr00018a003

543   Li, C., Wu, J., Peng, W., Fang, Z., Liu, J., 2019. Peroxymonosulfate activation for efficient

544   sulfamethoxazole degradation by Fe3O4/β-FeOOH nanocomposites: Coexistence of

545   radical and non-radical reactions. Chem. Eng. J. 356, 904–914.

546   https://doi.org/10.1016/j.cej.2018.09.064

547   Li, W., Zhang, Y., Liu, Y., Cheng, X., Tang, W., Zhao, C., Guo, H., 2019. Kinetic performance

548   of peroxymonosulfate activated by Co/Bi25FeO40: radical and non-radical mechanism. J.

549   Taiwan Inst. Chem. Eng. 100, 56–64. https://doi.org/10.1016/J.JTICE.2019.02.033

550   Liu, J., Zhou, J., Ding, Z., Zhao, Z., Xu, X., Fang, Z., 2017. Ultrasound irritation enhanced

551   heterogeneous activation of peroxymonosulfate with Fe3O4 for degradation of azo dye.

552   Ultrason. Sonochem. 34, 953–959. https://doi.org/10.1016/j.ultsonch.2016.08.005

553   Luo, Y., Guo, W., Ngo, H.H., Nghiem, L.D., Hai, F.I., Zhang, J., Liang, S., Wang, X.C., 2014.

554   A review on the occurrence of micropollutants in the aquatic environment and their fate

555   and removal during wastewater treatment. Sci. Total Environ. 473–474, 619–641.

556   https://doi.org/10.1016/j.scitotenv.2013.12.065

557   Mahdi-Ahmed, M., Chiron, S., 2014. Ciprofloxacin oxidation by UV-C activated

558   peroxymonosulfate in wastewater. J. Hazard. Mater. 265, 41–46.

559   https://doi.org/10.1016/j.jhazmat.2013.11.034

560   Mecha, A.C., Onyango, M.S., Ochieng, A., Momba, M.N.B., 2016. Impact of ozonation in

561   removing organic micro-pollutants in primary and secondary municipal wastewater: Effect

562   of process parameters. Water Sci. Technol. 74, 756–765.

563   https://doi.org/10.2166/wst.2016.276

564   Monteagudo, J.M., El-taliawy, H., Durán, A., Caro, G., Bester, K., 2018. Sono-activated

565   persulfate oxidation of diclofenac: Degradation, kinetics, pathway and contribution of the

566   different radicals involved. J. Hazard. Mater. 357, 457–465.

567   https://doi.org/10.1016/j.jhazmat.2018.06.031

568   Neta, P., Huie, R.E., Ross, A.B., 1988. Rate Constants for Reactions of Inorganic Radicals in

569   Aqueous Solution. J. Phys. Chem. Ref. Data 17, 1027–1284.

570   https://doi.org/10.1063/1.555808

571   Neta, P., Huie, R.E., Ross, A.B., 1982. Rate·Constants for Reactions of Inorganic Radicals in

572   Aqueous Solution. J. Phys. Chem. Ref. Data 17, 1027–1284.

573   https://doi.org/10.1063/1.555978

574   Nunes, R.F., Tominaga, F.K., Borrely, S.I., Teixeira, A.C.S.C., 2020. UVA/persulfate-driven

575   nonylphenol polyethoxylate degradation: effect of process conditions. Environ. Technol.

576   (United Kingdom) 1–15. https://doi.org/10.1080/09593330.2020.1786166

577   Palharim, P.H., Graça, C.A.L., Teixeira, A.C.S.C., 2020. Comparison between UVA- and zero-

578   valent iron-activated persulfate processes for degrading propylparaben. Environ. Sci.

579   Pollut. Res. 27, 22214–22224. https://doi.org/10.1007/s11356-020-08141-4

580   Peleyeju, M.G., Arotiba, O.A., 2018. Recent trend in visible-light photoelectrocatalytic systems

581   for degradation of organic contaminants in water/wastewater. Environ. Sci. Water Res.

Technol. https://doi.org/10.1039/c8ew00276b

Pera-Titus, M., García-Molina, V., Baños, M.A., Giménez, J., Esplugas, S., 2004. Degradation
of chlorophenols by means of advanced oxidation processes: A general review. Appl.
Catal. B Environ. 47, 219–256. https://doi.org/10.1016/j.apcatb.2003.09.010

Qi, W., Zhu, S., Shitu, A., Ye, Z., Liu, D., 2020. Low concentration peroxymonosulfate and
UVA-LED combination for E. coli inactivation and wastewater disinfection from
recirculating aquaculture systems. J. Water Process Eng. 36.
https://doi.org/10.1016/j.jwpe.2020.101362

Qi, Y., Qu, R., Liu, J., Chen, J., Al-Basher, G., Alsultan, N., Wang, Z., Huo, Z., 2019.
Oxidation of flumequine in aqueous solution by UV-activated peroxymonosulfate:
Kinetics, water matrix effects, degradation products and reaction pathways. Chemosphere
237, 124484. https://doi.org/10.1016/j.chemosphere.2019.124484

Rasoulifard, M.H., Fazli, M., Eskandarian, M.R., 2015. Performance of the light-emitting-
diodes in a continuous photoreactor for degradation of Direct Red 23 using UV-
LED/S2O82- process. J. Ind. Eng. Chem. 24, 121–126.
https://doi.org/10.1016/j.jiec.2014.09.018

Rizzo, L., Agovino, T., Nahim-Granados, S., Castro-Alférez, M., Fernández-Ibáñez, P., Polo-
López, M.I., 2019. Tertiary treatment of urban wastewater by solar and UV-C driven
advanced oxidation with peracetic acid: Effect on contaminants of emerging concern and
antibiotic resistance. Water Res. 149, 272–281.
https://doi.org/10.1016/j.watres.2018.11.031

Rodríguez-Chueca, Jorge, Guerra-Rodríguez, S., Raez, J.M., López-Muñoz, M.J.M.-J.M.J.,
Rodríguez, E., 2019. Assessment of different iron species as activators of S 2 O 82- and
HSO 5 - for inactivation of wild bacteria strains. Appl. Catal. B Environ. 248, 54–61.
https://doi.org/10.1016/j.apcatb.2019.02.003

607   Rodríguez-Chueca, J., Laski, E., García-Cañibano, C., Martín de Vidales, M.J., Encinas, Kuch,

608   B., Marugán, J., Rodríguez-Chueca, Laski, E., García-Cañibano, C., Martín de Vidales,

609   M.J., Encinas, Kuch, B., Marugán, J., Rodríguez-Chueca, J., Laski, E., García-Cañibano,

610   C., Martín de Vidales, M.J., Encinas, Á., Kuch, B., Marugán, J., Rodríguez-Chueca, Laski,

611   E., García-Cañibano, C., Martín de Vidales, M.J., Encinas, Kuch, B., Marugán, J.,

612   Encinas, Á., Kuch, B., Marugán, J., Encinas, Kuch, B., Marugán, J., 2018. Micropollutants

613   removal by full-scale UV-C/sulfate radical based Advanced Oxidation Processes. Sci.

614   Total Environ. 630, 1216–1225. https://doi.org/10.1016/j.scitotenv.2018.02.279

615   Rodríguez-Chueca, J, Varella della Giustina, S., Rocha, J., Fernandes, T., Pablos, C., Encinas,

616   Á., Barceló, D., Rodríguez-Mozaz, S., Manaia, C.M., Marugán, J., 2019. Assessment of

617   full-scale tertiary wastewater treatment by UV-C based-AOPs: Removal or persistence of

618   antibiotics and antibiotic resistance genes? Sci. Total Environ. 652, 1051–1061.

619   https://doi.org/10.1016/j.scitotenv.2018.10.223

620   Rubirola, A., Boleda, M.R., Galceran, M.T., 2017. Multiresidue analysis of 24 Water

621   Framework Directive priority substances by on-line solid phase extraction-liquid

622   chromatography tandem mass spectrometry in environmental waters. J. Chromatogr. A

623   1493, 64–75. https://doi.org/10.1016/j.chroma.2017.02.075

624   Sharma, J., Mishra, I.M., Dionysiou, D.D., Kumar, V., 2015. Oxidative removal of bisphenol a

625   by uv-c/peroxymonosulfate (pms): Kinetics, influence of co-existing chemicals and

626   degradation pathway. Chem. Eng. J. 276, 193–204.

627   https://doi.org/10.1016/j.cej.2015.04.021

628   Sousa, J.C.G., Ribeiro, A.R., Barbosa, M.O., Pereira, M.F.R., Silva, A.M.T., 2018. A review on

629   environmental monitoring of water organic pollutants identified by EU guidelines. J.

630   Hazard. Mater. 344, 146–162. https://doi.org/10.1016/J.JHAZMAT.2017.09.058

631   Sousa, J.C.G., Ribeiro, A.R., Barbosa, M.O., Ribeiro, C., Tiritan, M.E., Pereira, M.F.R., Silva,

632 A.M.T., 2019. Monitoring of the 17 EU Watch List contaminants of emerging concern in

633 the Ave and the Sousa Rivers. Sci. Total Environ. 649, 1083–1095.

634 https://doi.org/10.1016/J.SCITOTENV.2018.08.309

635 Stathoulopoulos, A., Mantzavinos, D., Frontistis, Z., 2020. Coupling persulfate-based AOPs: A

636 novel approach for piroxicam degradation in aqueous matrices. Water (Switzerland) 12.

637 https://doi.org/10.3390/W12061530

638 Valentín, L., Nousiainen, A., Mikkonen, A., 2013. Introduction to Organic Contaminants in

639 Soil: Concepts and Risks, Handbook of Environmental Chemistry.

640 https://doi.org/10.1007/698_2012_208

641 Venieri, D., Karapa, A., Panagiotopoulou, M., Gounaki, I., 2020. Application of activated

642 persulfate for the inactivation of fecal bacterial indicators in water. J. Environ. Manage.

643 261. https://doi.org/10.1016/j.jenvman.2020.110223

644 Vieira, O., Ribeiro, R.S., Pedrosa, M., Lado Ribeiro, A.R., Silva, A.M.T., 2020. Nitrogen-doped

645 reduced graphene oxide – PVDF nanocomposite membrane for persulfate activation and

646 degradation of water organic micropollutants. Chem. Eng. J. 402, 126117.

647 https://doi.org/10.1016/j.cej.2020.126117

648 Wang, J., Wang, S., 2018. Activation of persulfate (PS) and peroxymonosulfate (PMS) and

649 application for the degradation of emerging contaminants. Chem. Eng. J. 334, 1502–1517.

650 https://doi.org/10.1016/j.cej.2017.11.059

651 Wang, J., Zhuan, R., 2020. Degradation of antibiotics by advanced oxidation processes: An

652 overview. Sci. Total Environ. 701, 135023.

653 https://doi.org/10.1016/J.SCITOTENV.2019.135023

654 Wang, Q., Rao, P., Li, G., Dong, L., Zhang, X., Shao, Y., Gao, N., Chu, W., Xu, B., An, N.,

655 Deng, J., 2020. Degradation of imidacloprid by UV-activated persulfate and

656   peroxymonosulfate processes: Kinetics, impact of key factors and degradation pathway.

657   Ecotoxicol. Environ. Saf. 187, 109779. https://doi.org/10.1016/j.ecoenv.2019.109779

658 Wang, X., Brigante, M., Dong, W., Wu, Z., Mailhot, G., 2020. Degradation of Acetaminophen

659   via UVA-induced advanced oxidation processes (AOPs). Involvement of different radical

660   species: HO[rad], SO4[rad]− and HO2[rad]/O2[rad]−. Chemosphere 258.

661   https://doi.org/10.1016/j.chemosphere.2020.127268

662 Wei, M., Gao, L., Li, J., Fang, J., Cai, W., Li, X., Xu, A., 2016. Activation of

663   peroxymonosulfate by graphitic carbon nitride loaded on activated carbon for organic

664   pollutants degradation. J. Hazard. Mater. 316, 60–68.

665   https://doi.org/10.1016/j.jhazmat.2016.05.031

666 Xia, D., Li, Y., Huang, G., Yin, R., An, T., Li, G., Zhao, H., Lu, A., Wong, P.K., 2017.

667   Activation of persulfates by natural magnetic pyrrhotite for water disinfection: Efficiency,

668   mechanisms, and stability. Water Res. 112, 236–247.

669   https://doi.org/10.1016/j.watres.2017.01.052

670 Xie, P., Zhang, L., Chen, J., Ding, J., Wan, Y., Wang, S., Wang, Z., Zhou, A., Ma, J., 2019.

671   Enhanced degradation of organic contaminants by zero-valent iron/sulfite process under

672   simulated sunlight irradiation. Water Res. 149, 169–178.

673   https://doi.org/10.1016/j.watres.2018.10.078

674 Xu, H., Jiang, N., Wang, D., Wang, L., Song, Y., Chen, Z., Ma, J., Zhang, T., 2020. Improving

675   PMS oxidation of organic pollutants by single cobalt atom catalyst through hybrid radical

676   and non-radical pathways. Appl. Catal. B Environ. 263, 118350.

677   https://doi.org/10.1016/J.APCATB.2019.118350

678 Xu, X., Chen, J., Qu, R., Wang, Z., 2017. Oxidation of Tris (2-chloroethyl) phosphate in

679   aqueous solution by UV-activated peroxymonosulfate: Kinetics, water matrix effects,

680   degradation products and reaction pathways. Chemosphere 185, 833–843.

681   https://doi.org/10.1016/j.chemosphere.2017.07.090

682   Zanias, A., Frontistis, Z., Vakros, J., Arvaniti, O.S., Ribeiro, R.S., Silva, A.M.T., Faria, J.L.,

683   Gomes, H.T., Mantzavinos, D., 2020. Degradation of methylparaben by sonocatalysis

684   using a Co–Fe magnetic carbon xerogel. Ultrason. Sonochem. 64, 105045.

685   https://doi.org/10.1016/j.ultsonch.2020.105045

686   Zhang, X., Yao, J., Zhao, Z., Liu, J., 2019. Degradation of haloacetonitriles with

687   UV/peroxymonosulfate process: Degradation pathway and the role of hydroxyl radicals.

688   Chem. Eng. J. 364, 1–10. https://doi.org/10.1016/j.cej.2019.01.029

689   Zrinyi, N., Pham, A.L.-T., 2017. Oxidation of benzoic acid by heat-activated persulfate: Effect

690   of temperature on transformation pathway and product distribution. Water Res. 120, 43–

691   51. https://doi.org/10.1016/j.watres.2017.04.066

692

693　**Table captions**

694　**Table 1.** Studies involving the degradation of organic pollutants using UV-A activated persulfate

695　(PS).

696　**Table 2.** Characterization of the secondary treated wastewater used in this study.

697　**Table 4.** Number of germinated seeds of each specie in the phytotoxicity test

698　*Table 3. Micropollutants removal in non-spiked wastewater by PMS-UV-A, after 30 min of*

699　*reaction.*

700

Figure captions

702　**Figure 1.** Removal (%) of the target 20 multi-class MPs by PMS/UV-A, by varying the

703　concentration of PMS (0.05, 0.1 and 0.5 mM). Experimental conditions: Sample = WW spiked at

704　100 µg L^{-1}; pH = 7.6 (natural pH); Irradiation = 4 LEDs; Reaction time = 60 min.

705　**Figure 2**. Determination of the synergistic effects between PMS and UV-A radiation on the

706　degradation of the target 20 multi-class MPs: A) Removal by PMS/UV-A, PMS or UV-A (%) B)

707　Extent of synergy in the PMS/UV-A treatment, estimated for those MPs marked in Figure (A)

708　with an *. Experimental conditions: Sample = WW spiked at 100 µg L^{-1}; pH = 7.6 (natural pH);

709　Irradiation (when used) = 4 LEDs; [PMS] = 0.1 mM; Reaction time = 60 min.

710　**Figure 3.** Removals of a) Antibiotics; b) Beta-Blockers; c) Other pharmaceuticals; d) Herbicides;

711　and e) Insecticides. Experimental conditions: Sample = WW spiked at 100 µg L^{-1}; pH = 7.6

712　(natural pH); Irradiation = 4 LEDs; [PMS] = 0.1 mM.

713　**Figure 4.** PMS consumption during PMS/UV-A treatment. Experimental conditions: Sample =

714　WW spiked at 100 µg L^{-1}; pH = 7.6 (natural pH); Irradiation = 4 LEDs; [PMS] = 0.1 mM.

715　**Figure 5.** Removal (%) of MPs by PMS/UV-A, PMS, and PMS/UV-A in the presence of residual

716　ethanol (0.1%): effect of the presence of ethanol (EtOH). Experimental conditions: Sample = WW

717　spiked at 100 µg L^{-1}; pH = 7.6 (natural pH); Irradiation (when used) = 4 LEDs; [PMS] = 0.1 mM;

718　Time = 60 min.

719　**Figure 6.** Additional length increase (%) of roots and stems of three species (*Sorghum*

720　*Saccharatum, Sinapis alba, and Lepidium Sativum*) fed with PMS/UV-A treated wastewater, in

721　comparison to untreated wastewater.

722